



Stabilization heat treatment and functional response of 0.65[Pb(Mg_{1/3}Nb_{2/3})O₃]-0.35[PbTiO₃] ceramics

Pius Augustine^{a,b,c,*}, Shibnath Samanta^d, Martando Rath^a, Muralidhar Miryala^c, K. Sethupathi^d, Masato Murakami^c, M.S. Ramachandra Rao^{a,*}

^a Department of Physics, Nano Functional Material Technology Centre and Material Science Research Centre, Indian Institute of Technology Madras, Chennai, 600036, India

^b Department of Physics, Sacred Heart College (Autonomous), Kochi, 682013, India

^c Superconducting Materials Laboratory, Graduate School of Science and Engineering, Shibaura Institute of Technology 3-7-5 Toyosu, Koto-ku, Tokyo, 135-8548, Japan

^d Department of Physics, Low Temperature Physics Lab, Indian Institute of Technology Madras, Chennai, 600036, India

ARTICLE INFO

Article history:

Received 13 May 2017

Received in revised form 10 July 2017

Accepted 14 July 2017

Available online 17 July 2017

Keywords:

A. Ceramics

B. Microstructure

B. Piezoelectricity

D. Ferroelectricity

D. Dielectric properties

ABSTRACT

We report on the heat treatment to stabilize 0.65[Pb(Mg_{1/3}Nb_{2/3})O₃]-0.35[PbTiO₃] ceramics and its effect on the functional response. The stabilization heat treatment at 1050 °C for 4 h was effective in removing un-reacted PbO from the ceramics, which was confirmed through the measurements of dielectric and ferroelectric properties for a series of samples with different PbO contents. We also found that the stage of the stabilization heat treatment affected the sample properties. When this treatment was administered to the sample during calcination, it exhibited excellent ferroelectric behavior. On the other hand, the same stabilization heat treatment given to the compacted pellet prior to sintering resulted in excellent dielectric properties with comparatively low ferroelectric hysteresis.

© 2017 Elsevier Ltd. All rights reserved.

1. Introduction

Relaxor ferroelectrics are unique materials that exhibit dielectric dispersion with frequency, and attract special attention due to the excellent electromechanical energy conversion ability [1]. The compounds with chemical composition of (1-x)[Pb(Mg_{1/3}Nb_{2/3})O₃]-x[PbTiO₃] are pseudo-binary relaxor ferroelectric materials with excellent piezoelectric, dielectric, and ferroelectric properties, which will be attractive for applications like electromechanical actuators and sensors [2,3]. The (1-x) [Pb(Mg_{1/3}Nb_{2/3})O₃]-x [PbTiO₃] compound along the morphotropic phase boundary (x=0.30 to 0.36) are expected to show unusual properties due to complex crystal symmetry [2]. The composition with x=0.35 has been identified to show improved functional response and higher recoverable energy [4]. Despite their attractive properties, commercial utilization of these materials was restricted by the difficulty in synthesizing phase-pure and device-worthy PMN-PT

ceramics. The formation of secondary paraelectric pyrochlore phase destabilizes the perovskite phase and degrades its inherent properties, making it unsuitable for practical applications [5,6]. The loss in lead during the reaction between PbO and Nb₂O₅ was reported to be the possible reason for the formation of cubic and paraelectric secondary phase [7]. Columbite B-site precursor method along with a modulated heating pattern, facilitated the realization of phase pure and device worthy PMN-PT ceramics. Although stoichiometric and single phase PMN-PT ceramic could be realized through partial covering method combined with modulated heating [8], the stoichiometric target did not yield expected results in the growth of thin film using PLD. It was found that excess amount of PbO in the initial precursor was inevitable in suppressing the intrusion of the secondary phase, which was in good agreement with previous studies [6,9]. On the other hand, if the unreacted conducting PbO is segregated along the grain boundary, functional response of the ceramic system will be significantly affected [8]. This report presents an extensive study on the heat stabilization methods for realizing device worthy 0.65PMN-0.35PT ceramics, for ceramic applications and as target for thin film growth using pulsed laser deposition.

Earlier reports on the synthesis of PMN-PT perovskite through solid state reaction adopted a calcination of thoroughly mixed

* Corresponding authors at: Department of Physics, Nano Functional Material Technology Centre and Material Science Research Centre, Indian Institute of Technology Madras, Chennai, 600036, India.

E-mail addresses: piustine@gmail.com (P. Augustine), mrrao@iitm.ac.in (M.S. Ramachandra Rao).

precursors PbO, MgNb_2O_6 and TiO_2 at 850°C [9], in order to prevent the evaporation of PbO [10]. Stabilization of perovskite PMN-PT at a higher temperature (1050°C) would yield a high quality ceramic and can remove the excess and unreacted PbO in the ceramic after calcination. A slow heating rate up to 1050°C , after calcination at 850°C for 6 h, would facilitate the completion of the formation of perovskite structure. The perovskite phase so formed was further retained at 1050°C for 4 h, which is called the stabilization heat treatment (depicted in graphical abstract). Since the melting point of PMN-PT phase is above 1280°C , stabilization heating will not hamper the perovskite phase already formed, rather it will remove the unreacted PbO left in the sample and prevent its segregation along the grain boundary, leading to the enhancement of the electrical response of the ceramics. A thorough investigation on the effect of stabilization heating on the electric response of the PMN-PT ceramic compositions prepared, with and without excess PbO in the initial precursor is studied in this report. An attempt is also made to analyze the effect of stabilization heating on the properties of the ceramic compositions when applied to the sample in two different ways during synthesis.

2. Material and methods

2.1. Synthesis of PMN-PT ceramic

Ceramic synthesis was carried out using columbite B-site precursor route [10] and partial covering method [8,11]. Columbite-like MgNb_2O_6 precursor was prepared by mixing MgO (Aldrich 99+ %) and Nb_2O_5 (Alfa Aesar 99.9+ %) using an agate mortar and pestle followed by calcination at 1100°C for 6 h. An excess of 4% MgO was used to suppress the formation of secondary corundum-like, $\text{Mg}_4\text{Nb}_2\text{O}_9$, phase. Stoichiometric proportion of MgNb_2O_6 , PbO (Alfa Aesar 99.9+ %) and TiO_2 (Titanium (IV) oxide – Aldrich 99.8%) were thoroughly ground using a mortar and pestle and heat treated for phase formation using partial covering method coupled with modulated heating in a conventional furnace [8]. The samples were prepared by two methods where the stage of application of stabilization heat treatment is different. In the first batch, PMN-PT samples (S_1) were prepared with excess PbO from 0 to 12% (0%, 5%, 7%, 10% and 12%) in the precursor; and calcination at 850°C for 6 h was followed by stabilization heat treatment at 1050°C for 4 h, in order to study the effects of stabilization heat treatment on the exclusion of the unreacted PbO from the perovskite ceramics. In the second batch, PMN-PT samples (S_2) with excess PbO-7%, 10% and 12%, calcination was performed at 850°C for 6 h as in S_1 and the stabilization heating was applied on compacted pellet prior to sintering.

After calcination and phase confirmation using XRD, samples were compacted for densification. A thorough grinding of the calcined powder before making the pellet was given to all the samples to activate sintering kinetics at a relatively lower sintering

temperature (1150°C) for 4 h. All the pellet samples of ~ 12 mm diameter and ~ 1 mm thickness were prepared by applying a uniaxial pressure of 350 MPa for 5 min on hydraulic press under ambient conditions. The sintered pellets were annealed at 625°C for 30 min after the application of silver paste on either side [12], to depole the material and to relax the internal stresses that may have possibly been induced in the ceramic during preparation. Annealing would also ensure better adherence of metal on the oxide-ceramic layer and form stable electrode for temperature dependent electrical studies. XRD analysis was done in PANalytical Xpert Pro and Energy dispersive spectroscopy (EDS) imaging was carried out using JEOL 7100 FEG, Japan. Ferroelectric studies were performed using Radiant PE loop tracer (Radiant Technologies, USA) by placing the unpoled disc into silicone oil, and the dielectric studies were carried out in the frequency range 1.0 Hz to 100 kHz using Alpha High Resolution Dielectric/Impedance Analyzer (Novocontrol, Germany) (temperature increment was restricted to 5°C around T_m), for both S_1 and S_2 . Piezoelectric coefficient (d_{33}) was measured using a Piezo d_{33} meter (Sinocera-YE2730A) and microstructural morphology of the compositions was analyzed using HRSEM (Quanta 200 FEG scanning electron microscope). Density of the synthesized PMN-PT ceramics was determined using Archimedes' water displacement method. XPS analysis was carried out on sample prepared without using excess PbO to confirm the absence of secondary pyrochlore phase.

In the first section of the study (synthesis and analysis of sample S_1), the effects of stabilization heat treatment on the synthesis of phase-pure and device-worthy PMN-PT ceramics, with and without using excess PbO in the precursor, were analyzed through the measurements of dielectric and ferroelectric response exhibited by the ceramics.

In the second part, we studied the difference in functional response of the sample with 7% PbO when the stage to employ the stabilization heat treatment was changed. The effect of the stabilization time on the amount of excess PbO exclusion was also studied.

3. Results and discussion

3.1. X-ray diffractogram and EDS line scan

X-ray diffractogram of both S_1 and S_2 showed clean monophasic perovskite PMN-PT without any trace of pyrochlore phase or PbO phase (Fig. 1(ii)). Compositions S_1 and S_2 showed neither pseudo-cubic nor tetragonal crystal structure, but a mixed symmetry, which is evident from the study of FWHM and intensity ratios of the peak at $2\theta = 45^\circ$. Rietveld analysis on the composition (not shown) also confirmed the presence of mixed symmetry for the composition 0.65PMN-0.35PT. This is expected in the case of PMN-PT composition at the MPB.

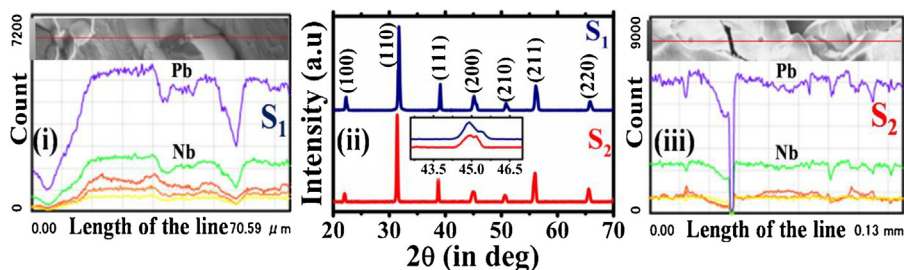


Fig. 1. (i) and (iii) EDS line scan image on S_1 and S_2 respectively. (No Pb deposition along the grain boundary), (ii) X-ray diffraction patterns of samples S_1 and S_2 . (Inset shows the peak profile at $2\theta = 45^\circ$).

Line scan was done on the bulk of the ceramic (Fig. 1(i) and 1(iii)) to ensure that no unused conducting Pb is deposited along the grain boundary as it will have adverse effect in the functional response of the system. Line scan profile did not exhibit any rise in count for Pb element at the grain boundary, which rule out the presence of Pb/PbO in the grain boundary and establish the efficacy of stabilization heating. Line scan were repeated at many sections of the same pellet as well as different pellets, to confirm the observations.

3.2. XRD – PbO exclusion and stabilization

XRD of PMN-PT pellet made with 12% excess PbO in the initial precursor (stabilization was given along with sintering) is shown in Fig. 2(i). Presence of PbO peaks in Fig. 2(i) indicates that stabilization heating applied could not eliminate unused PbO completely. When stabilization was given along with sintering, pellets made with excess PbO more than ~10% showed the presence of PbO reject which was clear from the coloration of the pellet and was confirmed from the XRD (Fig. 2). Pellets made with excess PbO 10% and below did not show the peaks corresponding to unreacted PbO phase in the XRD *i.e.* stabilization heating conditions optimized in the study was found to be effective in elimination of excess PbO upto 10% in the sample. All those pellets, which are made with excess PbO below 10% showed shining sandal yellow color, irrespective of whether stabilization heating was applied along with calcination or sintering.

Inset of Fig. 2(i) shows the photograph of the alumina dish in which the samples were calcined. It was found that, dish in which PMN-PT ceramic without excess PbO was stabilized, did not show any coloration (Fig. 2(i)(b)), where PbO expulsion was observed in the crucibles used for the calcination of samples having excess PbO (inset Fig. 2(i)). Absence of PbO deposit on the dish, in which the sample without excess PbO was calcined, is an indication that the entire PbO was used up in the phase formation and the final phase was not degraded at the heating conditions used for the sample stabilization [13,14]. However, when the stabilization temperature was further increased, coloration was observed, even in the crucible in which calcination of the sample without excess PbO was carried out. This could be because of the decomposition of the perovskite phase at higher temperature, and hence 1050 °C, was found to be an ideal choice for stabilization heating. So, the stabilization time may be modified according to the experimental requirement.

3.3. Energy dispersive X-ray spectroscopy (EDS) image

In order to confirm the phase purity of the ceramics and status of excess MgO used for the synthesis of columbite-like precursor MgNb_2O_6 , EDS imaging were carried out on the bulk of the samples S_1 and S_2 , which are shown in Fig. 3. Both the EDS measurements exhibited uniform distribution of elements in the measured area. To have better information, a broader area on the bulk region of the samples was selected for imaging. Uniform intensity of the image confirms the absence of secondary phase in the composition, which was noticed in XRD as well. However, both the EDS images of the samples S_1 and S_2 , showed small patches of intensity variations of Mg and O (Fig. 3), and this could be attributed to the expulsion of unused excess MgO, which was used for the synthesis of corundum-free columbite-like MgNb_2O_6 precursor. A smaller percentage (2% to 3%) of excess MgO, also would serve the purpose [8]. However, excess MgO did not cause any harm to the functional response of the ceramic as seen in the dielectric and ferroelectric response discussed.

3.4. X-ray photoelectron spectroscopy study of PMN-PT prepared without excess PbO

Fig. 4 shows the XPS spectra recorded for 0.65PMN-0.35PT pellet made without using excess PbO in the initial precursor. Core level spectrum of Pb exhibits spin orbit doublets with binding energies of 137.6 eV and 142.1 eV corresponding to $\text{Pb } 4f_{7/2}$ and $\text{Pb } 4f_{5/2}$ respectively. For single crystal PMN-PT, the elemental binding energy of Pb has been reported to be 136.9 eV [15] and the shift observed in this study is within the accepted limit of experimental and/or instrumental error. The fact that only one spin orbit doublet is seen for Pb rules out the possibility of multiple oxidation state for Pb in the composition.

Niobium core level spectrum shows spin orbit doublets of $3d_{5/2}$ at 205.5 eV and $3d_{3/2}$ at 208.1 eV respectively. The observed binding energies of the Nb doublets were in good agreement with the earlier reports on PMN-PT single crystal data [16] and correspond to the Nb^{5+} oxidation state, which is the expected value for pure PMN-PT perovskite phase. Since only one doublet spectrum is seen, and the oxidation state of Nb, that corresponds to pyrochlore phase (Nb^{4+}) [16] is not observed in the core spectrum, the XPS study confirms the absence of pyrochlore phase in the synthesized PMN-PT ceramic. Binding energy difference observed in Pb and Nb doublets are also consistent with the earlier reports [16,17].

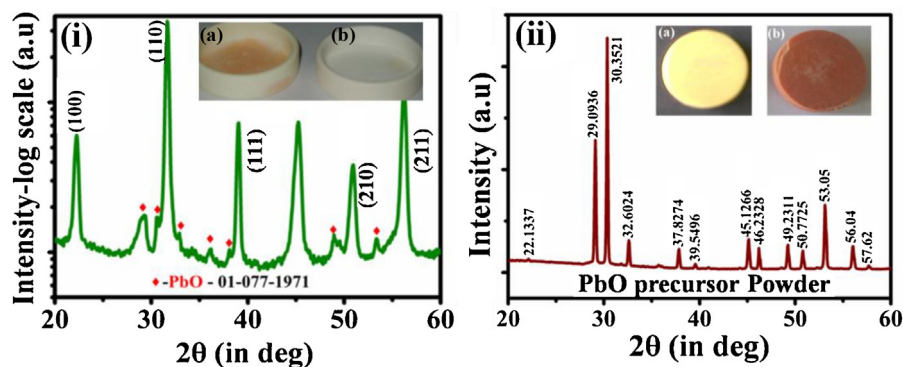


Fig. 2. (i) XRD of PMN-PT pellet made with 12% excess PbO in the initial precursor. (Stabilization was given along with sintering and i) shows the presence of PbO in the target) (ii) XRD of PbO precursor used for the synthesis of PMN-PT ceramic pellet.

[Inset photographs within Fig (i): (a) shows coloration in alumina dish, which was used for the calcination of the sample having excess PbO and (b) dish used for the calcination of stoichiometric sample. Inset photographs within Fig (ii): (a) pellet made with 12% excess PbO (stabilization heating along with calcination) and (b) pellet made with 12% excess PbO (stabilization heating along with sintering)].

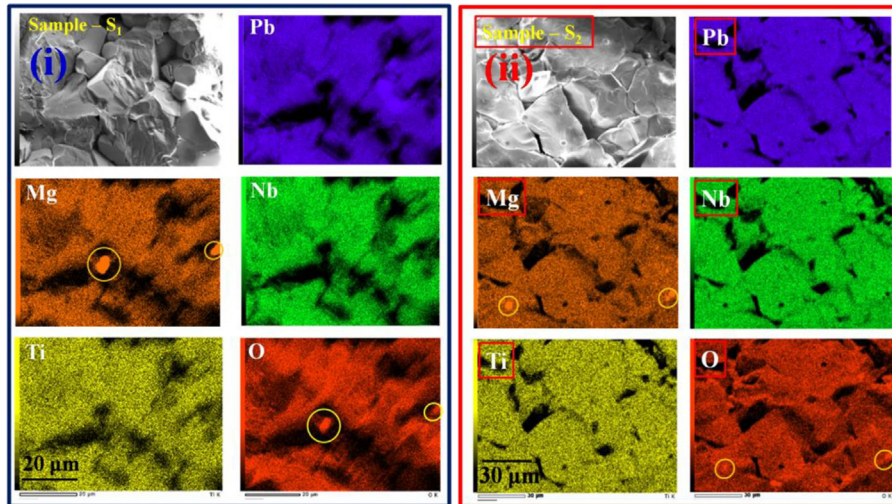


Fig. 3. Energy dispersive X-ray spectroscopy (EDS) image of (i) S_1 and (ii) S_2 . (MgO exclusion is shown in circle). Comparatively bigger grains are seen in S_2 .

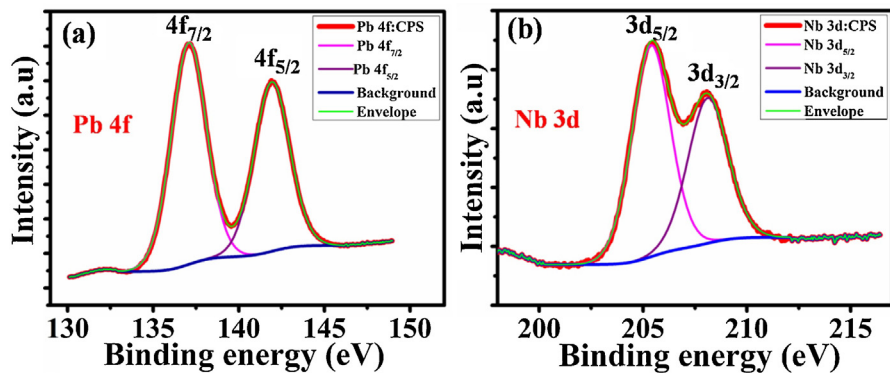


Fig. 4. XPS spectra for (a) Pb 4f and (b) Nb 3d levels, recorded for pure 0.65PMN-0.35PT pellet fabricated without using excess PbO in the initial precursor.

3.5. Part – 1: effectiveness of stabilization heating in eliminating excess PbO

3.5.1. Ferroelectric and differential permittivity study

Fig. 5 shows ferroelectric data for 0.65PMN-0.35PT which were prepared without using excess PbO and with 5% excess PbO in the precursor. All the samples were subjected to the stabilization heat treatment along with calcination, and exhibited almost similar ferroelectric properties, which could be due to the removal of the unreacted PbO during high temperature stabilization process. It was also evident from the microstructure and dielectric studies of the compositions. The highest P_r value is expected in the morphotropic phase boundary composition due to the summation of eight (111) rhombohedral polarization orientations with six (001) tetragonal orientations [18]. The relaxor ferroelectric behavior of the samples is quite evident from the value of the squareness factor (R_{sq}) (close to one) of the loops traced [19]. Creeping in hysteresis loop, which is generally expected due to the presence of PbO along the grain boundary in Pb-based ferroelectric systems, is not observed in our study. This further confirms the absence of unreacted PbO in the sintered ceramic.

To understand the dielectric response of the material with application of electric field, behavior of differential permittivity (calculated using IEEE Std-180–1986) was studied [Fig. 5(c) and 5 (d)]. As the field increases, differential permittivity shows a sharp increase initially and exhibits a maximum at or around coercive

field E_C . This demonstrates that under electric field E_C , most of the dipoles in the system get aligned. Beyond E_C , it is found that differential permittivity shows sharp reduction *i.e* further increase in the polarization is not possible. Beyond ≈ 10 kV/cm, differential permittivity remains nearly constant, as an outcome of which the saturation in polarization happens, and the same behavior is observed in P-E hysteresis measurement. Identical response observed with the compositions prepared with and without excess PbO is due to similarity in the polarizability of the compositions; and hence confirms the suitability of stabilization heating in realizing stoichiometric PMN-PT ceramic. Sharpness of the peak at a reasonably lower electric field is an indication of the better ferroelectric response of the system; and it may be attributed to an increase in the degree of tetragonality in the crystal symmetry at the end of morphotropic phase boundary ($x=0.35$).

3.5.2. Dielectric study-removal of unused excess PbO

Temperature variation of real part of dielectric permittivity (ϵ') at various frequencies for 0.65PMN-0.35PT prepared with and without excess PbO are shown in Fig. 6, which exhibits nearly identical dielectric permittivity and transition temperature T_C . Removal of unreacted PbO through stabilization heating prevents the segregation of conducting PbO along the grain boundary, which could be the reason for nearly identical dielectric response exhibited by the ceramic systems [20].

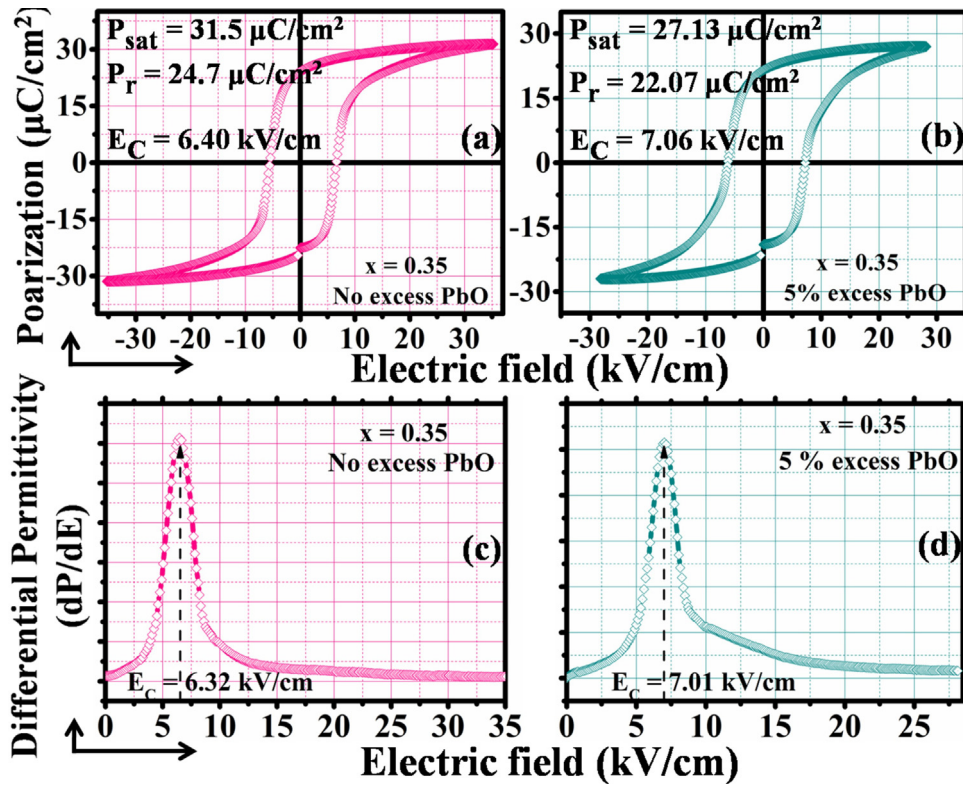


Fig. 5. Plots of ferroelectric hysteresis and differential permittivity: (a) and (b) ferroelectric hysteresis loops; and (c) and (d) variation of differential permittivity (dP/dE) with electric field exhibited by two compositions (prepared without using excess PbO and with 5% excess PbO in the precursor).

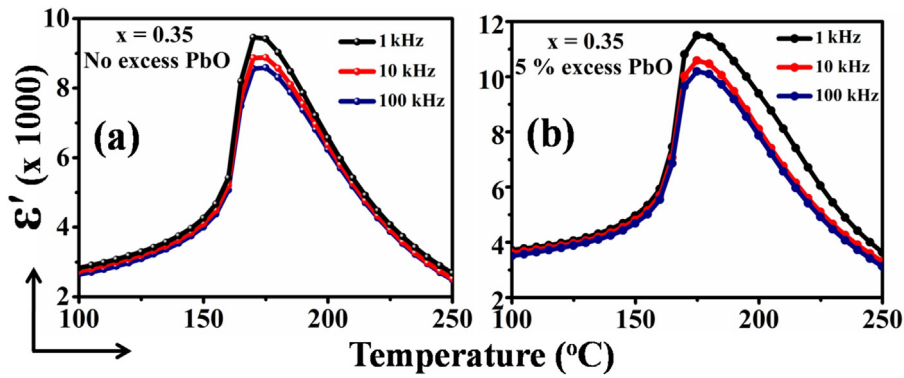


Fig. 6. Temperature variation of real part of dielectric permittivity (ϵ') at various frequencies for 0.65PMN-0.35PT (a) prepared without using excess PbO and (b) prepared using 5% excess PbO in the precursor.

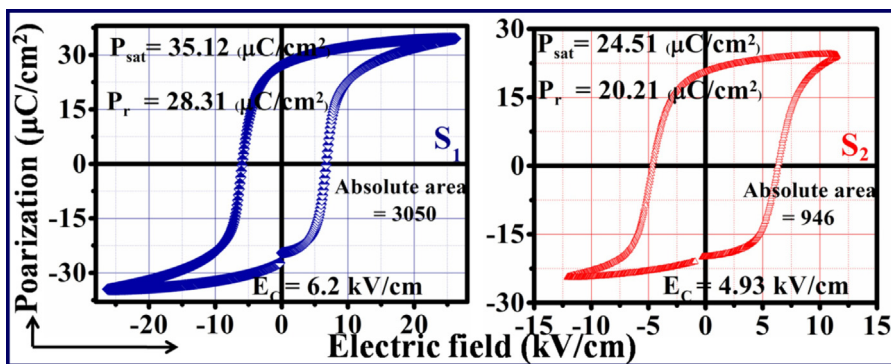


Fig. 7. Ferroelectric hysteresis loops traced for samples S_1 (stabilized with calcination) and S_2 (stabilized with sintering).

3.6. Part II effect of stabilization – along with calcination vs along with sintering

3.6.1. Ferroelectric response

It was observed that the ferroelectric loop traced by the sample S_1 (Fig. 7) shows higher values of saturation polarization ($P_{\text{sat}} = 35.12 \mu\text{C}/\text{cm}^2$), remnant polarization ($P_r = 28.31 \mu\text{C}/\text{cm}^2$), low coercive field ($E_c = 6.2 \text{ kV}/\text{cm}$), low leakage, and sharp tips; and hence may be suited for various ferroelectric device applications [21,22]. Ferroelectric response of sample S_2 are: saturation polarization ($P_{\text{sat}} = 24.51 \mu\text{C}/\text{cm}^2$), remnant polarization ($P_r = 20.21 \mu\text{C}/\text{cm}^2$) and low coercive field ($E_c = 4.93 \text{ kV}/\text{cm}$). Absolute area within the ferroelectric loop, is a measure of the ferroelectric strength of the ceramic which is given inset (S_1 –3050 and S_2 –946). Ferroelectric response obtained is correlated to microstructure of the ceramics which is included in the latter part of the report.

3.6.2. Dielectric response

The dielectric analysis exhibited a reverse trend in dielectric response. While the sample S_1 showed improved ferroelectric response, sample S_2 exhibited enhanced dielectric response. High dielectric permittivity (ϵ') and low loss factor ($\text{Tan } \delta$) (Fig. 8 and Table 1) establish superior dielectric behavior of sample S_2 compared to S_1 . A detailed account of the dielectric response exhibited by identical composition ($x = 0.35$) is available elsewhere [23–25]. Value of relaxor exponent, γ (>1.7) calculated for the samples attest a diffuse type first order ferroelectric-paraelectric phase transition [26]. The gradual increase in relaxor factor (γ) with increase in frequency observed in the sample S_2 (Table 1), was expected in a relaxor ferroelectric material, and may be attributed to dipole steering hysteresis [26]. T_m corresponding to ferroelectric-paraelectric phase transition, is found to be nearly equal for both the compositions S_1 and S_2 ($\sim 175^\circ\text{C}$), which was expected for the composition ($x = 0.35$) selected for the study [27]. Reductions in

Table 1

Dielectric behavior of samples S_1 and S_2 in the frequency range of 10 Hz to 100 kHz.

Frequency	ϵ_{max}		$\text{Tan}\delta_{\text{max}}$		γ	
	S_1	S_2	S_1	S_2	S_1	S_2
10 Hz	24816	25155	0.25	0.1	1.76	1.71
100 Hz	14039	21592	0.29	0.07	1.88	1.73
1 kHz	11057	20311	0.13	0.03	1.97	1.79
10 kHz	10387	19646	0.04	0.02	1.78	1.82
100 kHz	10057	19220	0.02	0.01	1.79	1.84

dipole moment observed beyond T_m may be attributed to the inverse dielectric response with temperature, which arise due to the relaxation time associated with the equilibrium alignment of the dipoles. Although, both the samples S_1 and S_2 exhibit excellent dielectric behavior comparable to earlier reports on this composition [24], reduction in the value of dielectric constant observed in S_1 compared to S_2 may be ascribed to the effect of stabilization heat treatment rather than defect dynamics [28]. In addition, superior dielectric response of S_2 makes it a favorable candidate for thin film development for integrated device applications, energy harvesting etc.

Since a prominent shift in T_m towards higher temperature with increasing frequency was not observed in the dielectric spectrum, the dielectric response of the samples was analyzed using Lorentz type relaxation behavior, details of which is available elsewhere [12,19,29,30]. A comparison of dielectric response of the two samples is shown in Table 1.

Dielectric response of the sample S_2 in the temperature range around T_c (Fig. 9(c)) shows the relaxor behavior of the ceramics prepared. At T_c ($\sim 175^\circ\text{C}$) dielectric constant shows maximum value in the entire range of frequency along which measurements were carried out. Also, for a particular value of the temperature, dielectric constant shows gradual reduction with increase in

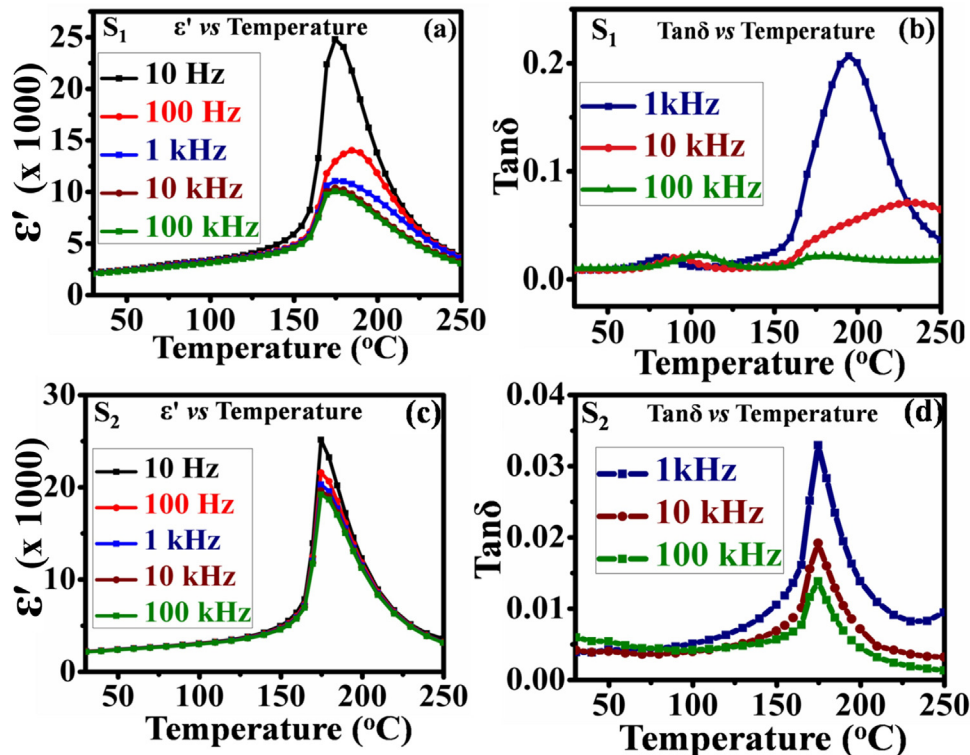


Fig. 8. Dielectric response: (a) and (c) Temperature dependence of real part of dielectric permittivity (ϵ'), (b) and (d) variation in $\text{Tan } \delta$ of sample S_1 and S_2 ; at various frequencies. ($\text{Tan } \delta$ values are shown only for higher frequencies).

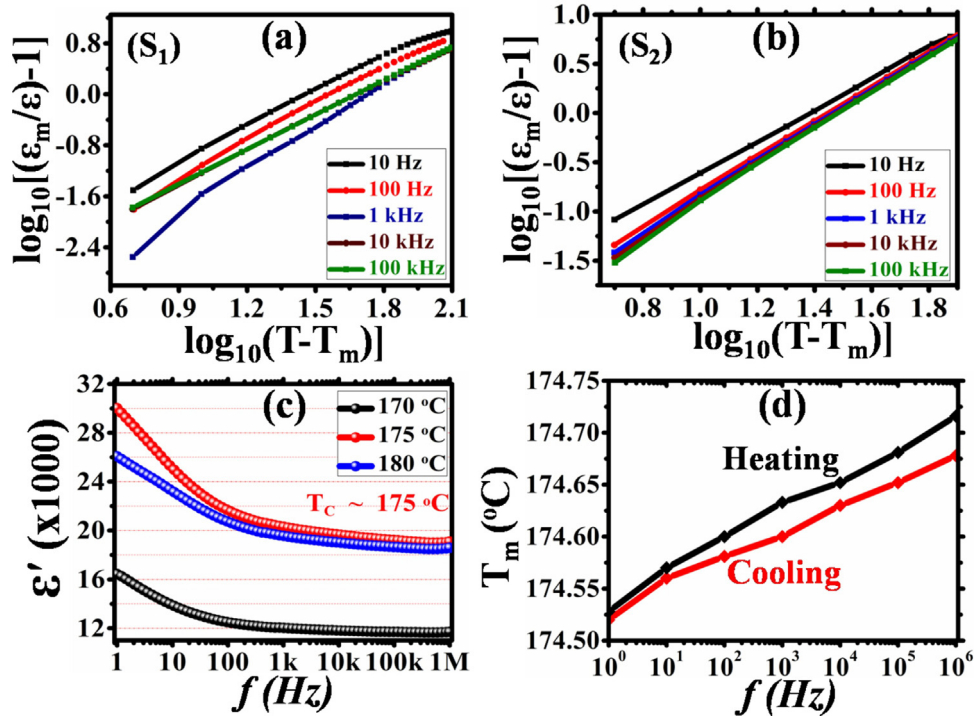


Fig. 9. Relaxation and thermal hysteresis: Variation of $\log_{10}[(\epsilon_m/\epsilon)-1]$ vs $\log_{10}(T-T_m)$ at various frequencies plotted for (a) S_1 and (b) S_2 . (c) Variation of real part of permittivity with frequency in the vicinity of transition temperature (shows relaxor behavior) (d) plot showing thermal hysteresis response exhibited by the sample S_2 .

frequency, which confirms the relaxor response of the ceramics. In order to make thermal hysteresis analysis of the composition, dielectric measurement of the sample (S_2) was carried out both during heating as well as cooling. Throughout the tested frequency range, dielectric permittivity showed only negligibly small shift during heating and cooling, as seen from the graph (Fig. 9(d)). Low thermal hysteresis observed during dielectric measurement confirms the device worthiness of the sample for piezoelectric applications.

3.6.3. Piezoelectric response

Piezoelectric coefficient d_{33} obtained at 24h after poling (370 pC/N and 452 pC/N respectively for the samples S_1 and S_2 respectively) establishes the device worthiness of the samples. Enhanced piezoresponse exhibited by S_2 may be attributed to higher dielectric constant, low dielectric loss and the easy mobility of polarization with low symmetry crystal structure (monoclinic Pm) at the MPB, which favors poling of the ceramics.

3.6.4. Microstructure study

Microstructure of the fractured surface of S_1 and S_2 exhibit enhanced grain growth (Fig. 10). Composition ($x=0.35$) is expected to have mixed crystal symmetry and an increase in the degree of tetragonality in the samples is quite evident from bigger size of the grains [27]. Higher P_r value of sample S_1 may be attributed to the presence of bimodal grains, which favors ferroelectric domain rotation or domain switching. Better squareness was expected for the composition ($x=0.35$) due to high proportion of PT and is an indication of the reduction in polar nano-domains in the ceramics, or conversion of nano-domains to micro-domains which results in increased domain size [31].

Superior ferroelectric behavior of S_1 could be attributed to the uniform distribution of bimodal grains ($\sim 10 \mu\text{m}$ and $4 \mu\text{m}$) throughout the sample [32] and the same is achieved due to the stabilization heating given along with calcination during synthesis, which cause increase in the tolerance factor and pushes the composition towards tetragonal symmetry. On the other hand, the

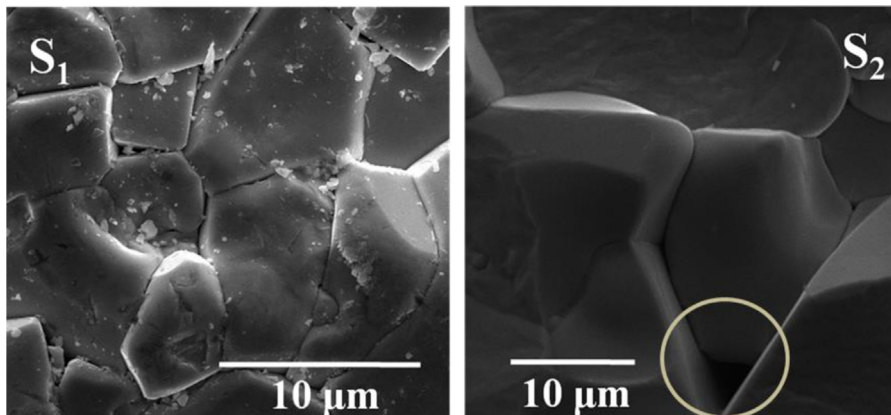


Fig. 10. Scanning electron micrographs of the fractured surfaces of the samples S_1 and S_2 .

sample S_2 exhibited comparatively reduced P_{sat} , P_r , E_c , and loses the symmetry of the tips of the bipolar hysteresis loop. Considerable reduction in E_c , which is observed in S_2 must be due to the increased grain size and is evident from the SEM micrograph. Larger grain growth in S_2 may be attributed to the presence of excess PbO in the green pellet, which on sintering lowers the average melting point and enhances the densification by easy mass transport and in turn expediting the rate of grain growth of the ceramics [33,34]. Increase in the grain size causes reduction in the grain boundaries, which are non polar, and in turn increase the dielectric constant and decrease the loss tangent [35]. Also, the increase in grain size may help to increase the domain size, which in turn reduces the pinning effect and may be responsible for the reduction in E_c observed in sample S_2 . However, the pores, which are seen in S_2 could be due to the nonuniform distribution and nonhomogeneous flow of PbO-rich liquid during sintering [36], which reduced the relative density of S_2 compared to S_1 (Relative density of S_1 and S_2 were $\sim 94\%$ and $\sim 91\%$ of theoretical density, respectively). Since the possibility of residual PbO along grain boundary in S_2 can be ruled out based on its dielectric behavior [14] and enhanced grain growth [37], reduction in ferroelectric response of S_2 may be due to the increased leakage current developed during hysteresis measurement owing to the presence of pores in the ceramic. Nearly identical squareness factor (R_{sq}) (close to one) and diffusiveness factor γ (close to two) of the samples S_1 and S_2 establish the relaxor nature of the PMN-PT ceramics synthesized.

We could prepare phase-pure thin films of PMN-PT from the high temperature stabilized and dense 0.65PMN-0.35PT target on $\text{La}_{0.5}\text{Sr}_{0.5}\text{CoO}_3$ buffered Pt/TiO₂/SiO₂/Si multilayer wafers using pulsed laser deposition, which also established the suitability of high temperature stabilization for the synthesis of PMN-PT like lead-based ceramics.

4. Conclusion

It has been found that stabilization heat treatment at 1050 °C for 4h was effective in synthesizing single-phase PMN-PT ceramic with high device quality. Exclusion of unreacted PbO from the ceramic with this treatment ensures clean grain boundary and high dielectric response. For ferroelectric applications, it is better to employ stabilization heating along with calcination. On the other hand, applying stabilization heating along with sintering was suitable for enhanced dielectric response. Relaxor exponent and squareness factor obtained in our study corroborate the relaxor response of the PMN-PT ceramic. Hence, it follows that the methods of heat stabilization described in the present study is efficient in the removal of unreacted excess PbO from the precursor and realization of PMN-PT. Our study establishes the feasibility of realizing phase pure PMN-PT without using excess PbO in the initial precursor and the device worthiness and functional response of high temperature stabilized ceramics.

Acknowledgments

MSR would like to thank (i) Department of Science and Technology (DST), New Delhi for providing the funding (SR/NM/NAT/02-2005) that facilitated the establishment of Nano Functional Materials Technology Centre (NFMTC) and (ii) DRDO (Project No: PHY/13-14/286/DRDO/MSRA). The paper was partly supported by the Japan Student Services Organization (JASSO), Shibaura Institute of Technology (SIT), under the Top Global University Project, designed by the Ministry of Education, Culture, Sports, Science and Technology of Japan.

Reference

- [1] S.E. Park, S. Eek, T.R. Shrout, Relaxor based ferroelectric single crystals for electro-mechanical actuators, *Mater. Res. Innovations* 1 (1) (1997) 20–25.
- [2] O. Bidault, E. Husson, A. Morell, Effects of lead vacancies on the spontaneous relaxor to ferroelectric phase transition in $\text{Pb}[(\text{Mg}_{1/3}\text{Nb}_{2/3})_0.9\text{Ti}_{0.1}]_3\text{O}_{13}$, *J. Appl. Phys.* 82 (1997) 5674–5679.
- [3] A.D. Hilton, D.J. Barber, C.A. Randal, T.R. Shrout, On short range ordering in the perovskite lead magnesium niobate, *J. Mater. Sci.* 5 (1990) 3461–3466.
- [4] Pius Augustine, M. Rath, M.S. Ramachandra Rao, Enhanced Functional Response of High Temperature Stabilized (1-x)pmn-xpt Ceramics, *Ceram. Int.* 43 (2017) 9408–9415.
- [5] Y.C. Liou, Stoichiometric perovskite PMN-PT ceramics produced by reaction-sintering process, *Mater. Sci. Eng. B* 103 (2003) 281–284.
- [6] S. Yu, H. Huang, L. Zhou, Y. Ye, A polyethylene glycol-Modified solid-State reaction route to synthesize relaxor ferroelectric $\text{Pb}(\text{Mg}_{1.8z}\text{Nb}_{2.8z}\text{O}_3)_{1-x}\text{PbTiO}_3$ (PMN-PT), *J. Am. Ceram. Soc.* 91 (4) (2008) 1057–1064.
- [7] S.L. Swartz, T.R. Shrout, Fabrication of perovskite lead magnesium niobate, *Mat. Res. Bull.* 17 (1982) 1245–1250.
- [8] Pius Augustine, M.S. Ramachandra Rao, Realization of device quality PMN-PT ceramics using modulated heating method, *Ceram. Int.* 41 (2015) 11984–11991.
- [9] C. Tantigate, J. Lee, A. Safari, Processing and properties of $\text{Pb}(\text{Mg}_{1.8z}\text{Nb}_{2.8z}\text{O}_3)_x\text{PbTiO}_3$ thin films by pulsed laser deposition, *Appl. Phys. Lett.* 66 (1995) 1610–1613.
- [10] H.C. Ling, M.F. Yan, Processing of lead based dielectric materials, in: B.I. Lee, E.J. A. Pope (Eds.), *Chemical Processing of Ceramics*, 1 eds., Marcel Dekker Inc., New York, 1994, pp. 397–419.
- [11] J. Kelly, M. Leonard, C. Tantigate, A. Safari, Effect of composition on the electromechanical properties of (1-x) $\text{Pb}(\text{Mg}_{1/3}\text{Nb}_{2/3})_3\text{O}_3$ -x PbTiO_3 ceramics, *J. Am. Ceram. Soc.* 80 (4) (1997) 957–964.
- [12] S. Ke, H. Fan, H. Huang, H.L.W. Chan, Lorentz-type relationship of the temperature dependent dielectric permittivity in ferroelectrics with diffuse phase transition, *Appl. Phys. Lett.* 93 (2008) 1–3 (112906).
- [13] S. Shah, M.S. Ramachandra Rao, Preparation and dielectric study of high-quality PLZT x/65/35 (x = 6,7,8) ferroelectric ceramics, *Appl. Phys. A* 71 (2000) 65–69.
- [14] D. Kušcer, M. Skalar, J. Holc, M. Kosec, Processing and properties of 0.65 $\text{Pb}(\text{Mg}_{1/3}\text{Nb}_{2/3})_3\text{O}_3$ -0.35 PbTiO_3 thick films, *J. Eur. Ceram. Soc.* 29 (2009) 105–113.
- [15] A. Kania, E. Talik, M. Kruzek, A. Słodczyk, Probing structural disorder in (1-x) $\text{PbMg}_{1/3}\text{Nb}_{2/3}\text{O}_3$ -x PbTiO_3 single crystals by x-ray photoelectron spectroscopy, *J. Phys. Cond. Matt.* 17 (2005) 6737–6750.
- [16] M. Grunder, J. Halbritter, XPS and AES studies on oxide growth and oxide coatings on niobium, *J. Appl. Phys.* 51 (1) (1980) 397–405.
- [17] E.-E. Latta, Maria Ronay, Catalytic oxidation of niobium, *Phys. Rev. Lett.* 53 (9) (1984) 948–951.
- [18] L. Ai, X. Li, Z. Wang, Y. Liu, C. He, T. Li, T. Chu, D. Pang, H. Tailor, X. Long, Preparation, structure, and electric properties of the $\text{Pb}(\text{Zn}_{1/3}\text{Nb}_{2/3})_3\text{O}_3$ - $\text{Pb}(\text{Yb}_{1/2}\text{Nb}_{1/2})_3\text{O}_3$ - PbTiO_3 ternary ferroelectric system ceramics near the morphotropic phase boundary, *J. European Cer. Soc.* 33 (2013) 2155–2165.
- [19] R. Cao, G. Li, J. Zeng, S. Zhao, L. Zheng, Q. Yin, The piezoelectric and dielectric properties of 0.3 $\text{Pb}(\text{Ni}_{1/3}\text{Nb}_{2/3})_3\text{O}_3$ -x PbTiO_3 -(0.7-x) PbZrO_3 ferroelectric ceramics near the morphotropic phase boundary, *J. Am. Ceram. Soc.* 93 (3) (2010) 737–741.
- [20] P. Ravindranathan, S. Komarneni, A.S. Bhalla, R. Roy, Synthesis and dielectric properties of solution sol-Gel-Derived 0.9 $\text{Pb}(\text{Mg}_{1.8z}\text{Nb}_{2.8z}\text{O}_3)_3\text{O}_3$ -0.1 PbTiO_3 ceramics, *J. Am. Ceram. Soc.* 74 (12) (1991) 2996–2999.
- [21] G.H. Haertling, Ferroelectric ceramics: history and technology, *J. Am. Ceram. Soc.* 82 (4) (1999) 797–818.
- [22] S. Patel, A. Chauhan, R. Vaish, Enhancing electrical energy storage density in anti-ferroelectric ceramics using ferroelastic domain switching, *Mater. Res. Express* 1 (2014) 1–12 (045502).
- [23] A.A. Bokov, Z.G. Ye, Phenomenological description of dielectric permittivity peak in relaxor ferroelectrics, *Solid State Commun.* 116 (2000) 105–108.
- [24] H. Uršič, M. Hrovat, J. Holc, J. Tellier, S. Drnovšek, N. Guiblin, B. Dkhil, M. Kosec, Influence of the substrate on the phase composition and electrical properties of 0.65 PMN-0.35 PT thick films, *J. Eur. Ceram. Soc.* 30 (2010) 2081–2092.
- [25] Z. Xia, L. Wang, W. Yan, Q. Li, Y. Zhang, Comparative investigation of structure and dielectric properties of $\text{Pb}(\text{Mg}_{1/3}\text{Nb}_{2/3})_3\text{O}_3$ - PbTiO_3 (65/35) and 10% PbZrO_3 -doped $\text{Pb}(\text{Mg}_{1/3}\text{Nb}_{2/3})_3\text{O}_3$ - PbTiO_3 (65/35) ceramics prepared by a modified precursor method, *Mat. Res. Bull.* 42 (2007) 1715–1722.
- [26] X. Chao, Z.M. Wang, Y. Tian, Y. Zhou, Z. Yang, $\text{Ba}(\text{Cu}_{0.5}\text{W}_{0.5})_3\text{O}_{13}$ -induced sinterability, electrical and mechanical properties of $(\text{Ba}_{0.85}\text{Ca}_{0.15}\text{Ti}_{0.90}\text{Zr}_{0.10})_3\text{O}_{13}$ ceramics sintered at low temperature, *Mat. Res. Bull.* 66 (2015) 16–25.
- [27] M. Alguero, J. Ricote, R. Jime'nez, P. Ramos, J. Carreaud, B. Dkhil, J.M. Kiat, J. Holc, M. Kosec, Size effect in morphotropic phase boundary $\text{Pb}(\text{Mg}_{1.8z}\text{Nb}_{2.8z}\text{O}_3)_3\text{O}_3$ - PbTiO_3 , *Appl. Phys. Lett.* 91 (2007) 1–3 (112905).
- [28] S. Zhao, Q. Li, Y. Feng, C. Nan, Microstructure and dielectric properties of PMN-PT ceramics prepared by the molten salts method, *J. Phys. Chem. Solids* 70 (2009) 639–644.
- [29] A. Słodczyk, P. Daniel, A. Kania, Local phenomena of (1-x) $\text{PbMg}_{1/3}\text{Nb}_{2/3}\text{O}_3$ -x PbTiO_3 single crystals ($0 \leq x \leq 0.38$) studied by raman scattering, *Phys. Rev. B* 14 (1981) 1–16.
- [30] Z. Xi, Q. Bu, P. Fang, W. Long, X. Li, Effect of frequency and temperature on dielectric relaxation of [111]-oriented PMN-32PT single crystals, *J. Alloys Compd.* 618 (2015) 14–18.

- [31] D. Viehland, M.C. Kim, J.F. Li, Long-time present tweed like precursors and paraelectric clusters in ferroelectrics containing strong quenched randomness, *Appl. Phys. Lett.* 67 (1995) 2471–2473.
- [32] J.C. Ho, K.S. Liu, I.N. Lin, Study of ferroelectricity in the PMN-PT system near the morphotropic phase boundary, *J. Mater. Sci.* 28 (1993) 4497–4502.
- [33] B. Fang, C. Ding, J. Wu, Q. Du, J. Ding, Effects of dopants on the synthesis of Pb (Mg_{1/3}Nb_{2/3}) O₃-PbTiO₃ ceramics by the reaction-sintering method, *Phys. Status Solidi A* 208 (2011) 1641–1645.
- [34] S. Fushimi, T. Ikeda, Phase equilibrium in the system PbO-TiO₂-ZrO₂, *J. Am. Ceram. Soc.* 50 (1967) 129–132.
- [35] M. Promsawat, A. Watcharapasorn, Z.G. Ye, S. Jiansirisomboon, Enhanced dielectric and ferroelectric properties of Pb(Mg_{1/3}Nb_{2/3})_{0.65}Ti_{0.35}O₃ ceramics by ZnO modification, *J. Am. Ceram. Soc.* 98 (3) (2014) 848–854.
- [36] Y.C. Zhang, Z.Z. Yang, W.N. Ye, C.J. Lu, L.H. Xia, Effect of excess pb on microstructures and electrical properties of 0.67 Pb (Mg_{1/3}Nb_{2/3}) O₃-0.33 PbTiO₃ceramics, *J. Mater. Sci. Mater. Electron.* 22 (2011) 309–314.
- [37] P. Ravindranathan, S. Komarneni, A.S. Bhalla, R. Roy, Synthesis and dielectric properties of solution sol-Gel-Derived 0.9Pb(Mg_{1&z.urule:3}Nb_{2&z.urule:3})O₃-0.1PbTiO₃ ceramics, *J. Am. Ceram. Soc.* 74 (12) (1991) 2996–2999.